Zero and one jet combined next-to-leading order analysis of the top quark forward-backward asymmetry

Stefan Höche, Junwu Huang, Gionata Luisoni, Jan Winter, and Marek Schönherr

Phys. Rev. D **88**, 014040 — Published 25 July 2013

DOI: 10.1103/PhysRevD.88.014040

Zero and one jet combined NLO analysis of the top quark forward–backward asymmetry

Stefan Höche* and Junwu Huang†
SLAC National Accelerator Laboratory, Menlo Park, CA 94025, USA

Gionata Luisoni‡ and Jan Winter§
Max-Planck Institut für Physik, Föhringer Ring 6, 80805 München, Germany

Marek Schönherr¶
Institute for Particle Physics Phenomenology, Durham University, Durham DH1 3LE, UK

We present an analysis of the forward–backward asymmetry in the production of top quark pairs at the Tevatron collider. We use novel Monte Carlo methods for merging matrix elements and parton showers to combine NLO QCD predictions for $t\bar{t}$ and $t\bar{t}$+jet production. Theoretical uncertainties are quantified in detail. We find agreement with experimental data on the transverse momentum dependence of the asymmetry.

I. INTRODUCTION

The forward–backward asymmetry in the production of top quark pairs offers great opportunities to study the physics both within and beyond the Standard Model (SM). At $p\bar{p}$ colliders, the asymmetry in dependence on the observable O is defined as

$$A_{\mathrm{FB}}(O) = \frac{\mathrm{d}\sigma_{t\bar{t}}/\mathrm{d}O|_{\Delta y>0} - \mathrm{d}\sigma_{t\bar{t}}/\mathrm{d}O|_{\Delta y<0}}{\mathrm{d}\sigma_{t\bar{t}}/\mathrm{d}O|_{\Delta y>0} + \mathrm{d}\sigma_{t\bar{t}}/\mathrm{d}O|_{\Delta y<0}}\,, \tag{1}$$

where $\Delta y = y_t - y_{\bar{t}}$ is the rapidity difference between the top and the antitop quark.

Unexpectedly large inclusive and differential asymmetries were found in various measurements at the Tevatron [1]. By now, both the CDF and DØ collaborations observed values that cannot be described by predictions based on the Standard Model [2–4]. The CDF collaboration has reported on forward–backward asymmetries at $\sqrt{s} = 1.96\,\mathrm{TeV}$ using the full Run II data set [5]. Their result was compared to theoretical predictions from various Monte Carlo event generators and next-to-leading order (NLO) calculations in the Standard Model. This analysis confirmed a discrepancy between theory and experiment which was observed earlier. It is most significant for those $t\bar{t}$ events with large invariant mass, $m_{t\bar{t}} \geq 450\,\mathrm{GeV}$. The inclusive parton-level asymmetry was measured as 0.164 ± 0.047 considering all pair masses, and 0.295 ± 0.067 for $m_{t\bar{t}} \geq 450\,\mathrm{GeV}$. This needs to be compared to theoretical predictions from various event generators in the unrestricted and high $t\bar{t}$ mass region: 0.067 ± 0.020 and 0.089 ± 0.027 from MC@NLO [6, 7], 0.066 ± 0.020 and 0.100 ± 0.030 from POWHEG [8, 9], and 0.073 ± 0.022 and 0.110 ± 0.033 from MCFM [4, 10]. In all cases, electroweak corrections had been applied. The linear behavior of A_{FB} with increasing Δy and $m_{t\bar{t}}$ persists, but the prediction for the slope is reduced by $\sim 2\,\sigma$ compared to earlier measurements for both the $m_{t\bar{t}}$ and the Δy dependence.

The observation of a large asymmetry has triggered substantial theoretical investigation. Various new physics models have been proposed to explain the discrepancy seen within the SM, such as $t\bar{t}$ production via a heavy axial color octet or a flavor changing Z' boson [11]. However, in order to ensure that the asymmetry is indeed a first hint of new physics beyond the Standard Model, a systematic study of QCD and Electroweak (EW) corrections at NLO and beyond must be performed to reduce theoretical uncertainties as much as possible. It was pointed out in [12] that color flows from incoming quarks to the top quark and from antiquarks to the antitop quark lead to more radiation when the top quark goes backward. This generates a positive asymmetry already at the level of parton showers that include color coherence effects. NLO QCD predictions for $t\bar{t}$ and $t\bar{t}$+jet [13, 14] exhibit a non-constant K-factor, such that additional effects are expected. Much attention has also been paid to the calculation of the EW contributions to the asymmetry from pure EW interactions and the interplay between EW and QCD processes [15]. A combined

* shoeche@slac.stanford.edu
† curlyh@stanford.edu
‡ luisonig@mpp.mpg.de
§ jwinter@mpp.mpg.de
¶ marek.schoenherr@durham.ac.uk

correction of 26% on top of the QCD prediction was determined at $O(\alpha_s^2\alpha)$ and $O(\alpha^2)$. Tremendous efforts have been recently made to complete the full NNLO QCD cross section calculation [16]. Soft-gluon resummation was also performed in this context [17].

It is important to note, that all general-purpose Monte Carlo event generators which are currently being used by experiments provide at most the inclusive prediction for $t\bar{t}$ production at the NLO matched to a parton shower [7, 9]. While calculations of $t\bar{t}$+jet production at NLO have been matched to parton showers independently [18], they have not yet been combined with the inclusive simulation of $t\bar{t}$ production in a manner that allows for improved predictions of $A_{\rm FB}$. We remedy this situation in the present publication, providing a merged simulation of $t\bar{t}$ and $t\bar{t}$+jet production at hadron colliders, which preserves both the NLO accuracy of the fixed-order prediction and the logarithmic accuracy of the parton shower. We are thus able to make predictions for both, the transverse momentum dependent asymmetry above a certain threshold and the inclusive asymmetries, which depend strongly on both, real and virtual higher-order QCD corrections. We do not include electroweak corrections in this publication, these can be inferred from [15].

We employ the MEPS@NLO technique for combining multiple NLO parton-level calculations with parton showers. The method was introduced in [19] and is implemented in the general-purpose event generator SHERPA [20]. Virtual corrections are computed using the GOSAM [21] package, which makes use of the program SAMURAI [22] based on integrand reduction techniques [23], and the tensor integral library GOLEM95 [24]. The interface between SHERPA and GOSAM [25] uses the Binoth–Les–Houches accord (BLHA) [26].

A fair amount of uncertainty is involved in parton-shower simulations of $A_{\rm FB}$, both inclusive and differential $A_{\rm FB}$ [12]. Some of these uncertainties will be eliminated by a combination of higher-multiplicity NLO calculations with the inclusive result. Some of them remain, such as the uncertainty related to the choice of exponent in the Sudakov factor of the parton shower. This has been discussed extensively in [27]. We do not attempt to systematically improve the parton shower here. Therefore, our ability to describe the inclusive asymmetry is still somewhat limited. However, we can quantify the possible impact of a systematic improvement at higher parton multiplicity by judging the impact of matrix-element plus parton-shower merging at the NLO. Moreover, we readily provide an NLO-accurate prediction for the transverse momentum dependent asymmetry for all but the first bin in $p_{T,t\bar{t}}$. [1]

The paper is organized as follows: Section II introduces the MC@NLO method, as implemented in SHERPA, and discusses color-coherence effects on $A_{\rm FB}$. Section III briefly reviews the MEPS@NLO technique and discusses related uncertainties. Section IV presents our final predictions, and Sec. V contains some concluding remarks.

II. MC@NLO FOR MASSIVE PARTICLES

The MC@NLO method is a modified subtraction scheme, which relies on the unitarity condition of the parton shower. Virtual corrections are approximated by the parton shower as the counterpart of real-emission corrections, integrated over the phase space of the emission. This implies that parton showers do not change the weight of a Monte Carlo event. They simply move events from the n-parton phase space to the $(n+1)$-parton phase space by means of branching processes.

Parton branching as implemented in MC@NLO can be described by the following equation, which determines the expectation value of an arbitrary, infrared-safe observable, denoted by O,

$$\langle O\rangle \;=\; \int \mathrm{d}\Phi_B\,\bar{\mathrm{B}}^{(\mathrm{A})}(\Phi_B)\,\mathcal{F}^{(\mathrm{A})}(\mu_Q^2,O) + \int \mathrm{d}\Phi_R\,\mathrm{H}^{(\mathrm{A})}(\Phi_R)\,\mathcal{F}_1(t,O)\;. \tag{2}$$

In this context,

$$\mathcal{F}^{(\mathrm{A})}(\mu_Q^2,O) \;=\; \Delta^{(\mathrm{A})}(t_c,\mu_Q^2)\,O(\Phi_B) + \int_{t_c}^{\mu_Q^2}\mathrm{d}\Phi_1\,\frac{\mathrm{D}^{(\mathrm{A})}(\Phi_B,\Phi_1)}{\mathrm{B}(\Phi_B)}\,\Delta^{(\mathrm{A})}(t,\mu_Q^2)\,\mathcal{F}_1(t,O) \tag{3}$$

is the generating functional of the MC@NLO, while $\mathcal{F}_n(t,O)$ denotes the generating functional of the parton shower. Φ_B and Φ_R denote the Born- and real-emission phase space, and Φ_1 is the phase space associated with the emission of an additional parton, i.e. $\mathrm{d}\Phi_R = \mathrm{d}\Phi_B\cdot\mathrm{d}\Phi_1$. It is parametrized in the standard manner as $\mathrm{d}\Phi_1 = \mathrm{d}t\,\mathrm{d}z\,\mathrm{d}\phi\,J(t,z)$, where t is called the evolution variable, z is called the splitting variable, ϕ is an azimuthal splitting angle and $J(t,z)$ is a Jacobian factor. Thus, where appropriate, $t\equiv t(\Phi_1)$ is understood. The functions $\bar{\mathrm{B}}^{(\mathrm{A})}$ and $\mathrm{H}^{(\mathrm{A})}$ are called the

[1] Note that this is a major difference between our results and the predictions from [28]. Other differences include the treatment of color (cf. Sec. II) and truncated shower effects (cf. Sec. III).

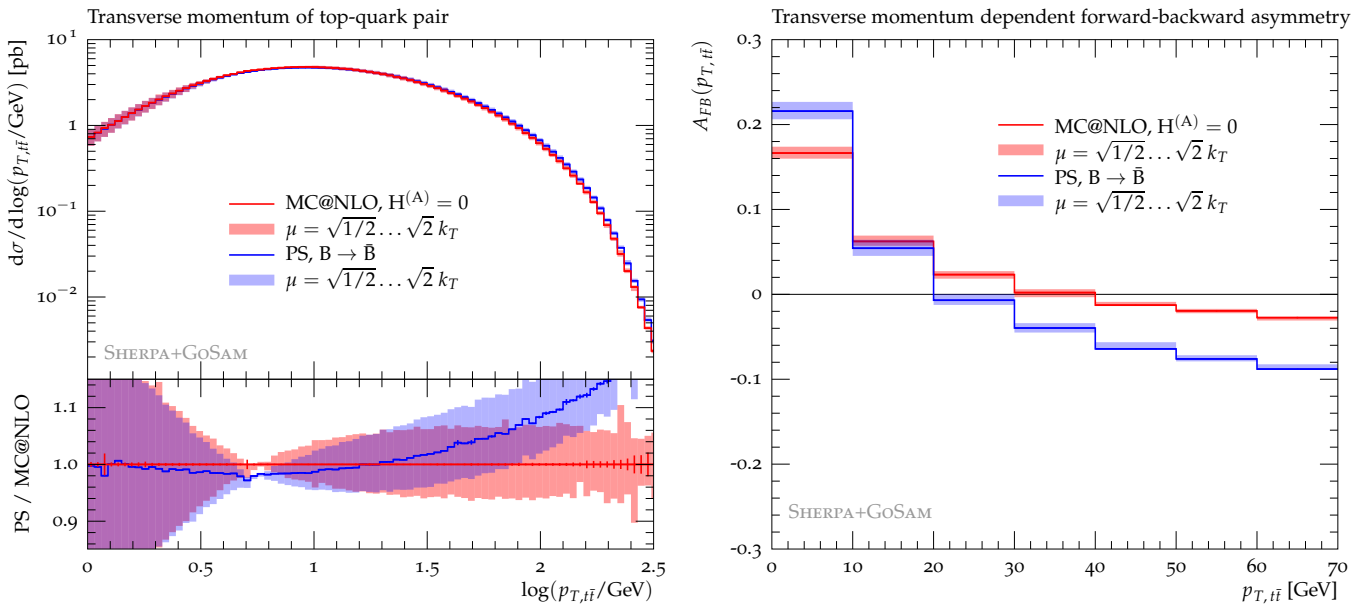

FIG. 1. Transverse momentum spectrum of the $t\bar{t}$ pair (left) and p_T-dependent forward–backward asymmetry (right). We compare the MC@NLO prediction (red) and the parton-shower result (blue). Hard remainder terms have been set to zero in the MC@NLO simulation, while the parton shower has been reweighted with the local K-factor $\bar{\mathrm{B}}^{(\mathrm{A})}/\mathrm{B}$ in order to make the two results comparable. Uncertainty bands stem from varying the scale of strong couplings in the resummation.

NLO-weighted Born differential cross section and the hard remainder function, defined as

$$\begin{aligned}\bar{\mathrm{B}}^{(\mathrm{A})}(\Phi_B) &= \mathrm{B}(\Phi_B) + \tilde{\mathrm{V}}(\Phi_B) + \mathrm{I}^{(\mathrm{S})}(\Phi_B) + \int \mathrm{d}\Phi_1 \left[\mathrm{D}^{(\mathrm{A})}(\Phi_B,\Phi_1)\,\Theta\left(\mu_Q^2 - t\right) - \mathrm{D}^{(\mathrm{S})}(\Phi_B,\Phi_1)\right], \\ \mathrm{H}^{(\mathrm{A})}(\Phi_R) &= \mathrm{R}(\Phi_R) - \mathrm{D}^{(\mathrm{A})}(\Phi_R)\,\Theta\left(\mu_Q^2 - t\right)\ .\end{aligned} \tag{4}$$

The terms B and R represent Born- and real-emission matrix elements, including flux and parton luminosity factors; $\mathrm{D}^{(\mathrm{S})}$ and $\mathrm{I}^{(\mathrm{S})}$ are the subtraction and integrated subtraction terms, respectively. $\tilde{\mathrm{V}}$ represents the virtual corrections, including collinear mass-factorization counterterms. $\mathrm{D}^{(\mathrm{A})}$ is the resummed part of the real-emission correction, which must approach R in both the collinear and the soft limit.

Within the event generator SHERPA, $\mathrm{D}^{(\mathrm{A})}$ is defined by the dipole subtraction terms employed in the method of Catani and Seymour (CS) [29]. Their phase space is restricted by the resummation scale μ_Q^2 [27]. The corresponding dipole insertion operators are modified such that their helicity summed splitting operator is positive definite, while negative values induced through spin dependence and color insertion operators are kept. Thus, spurious negative terms arising from arbitrary finite corrections are not resummed through $\mathrm{D}^{(\mathrm{A})}$.

So far, the MC@NLO method had been implemented only for massless partons in SHERPA. In the context of this work, we extended the implementation to massive partons, using kinematics and phase-space factorization in the method of Catani, Seymour, Dittmaier and Trocsanyi (CDST) [30]. The evolution variable is chosen to be a Lorentz invariant transverse momentum. Using the definitions of [29], for final-state branchings $\{\widetilde{ij},\tilde{k}\} \to \{i,j,k\}$ we have (denoting parton masses by m)

$$t^{(\mathrm{FS})} \;=\; 2\,p_i p_j\,\tilde{z}_{i,jk}(1-\tilde{z}_{i,jk}) - (1-\tilde{z}_{i,jk})^2\,m_i^2 - \tilde{z}_{i,jk}^2\,m_j^2\ , \tag{5}$$

while for initial-state branchings $\{\widetilde{aj},\tilde{k}\} \to \{a,j,k\}$ we use

$$t^{(\mathrm{IS})} \;=\; 2\,p_a p_j\,(1-x_{aj,k})\ . \tag{6}$$

Note that these definitions are independent of the type of the spectator parton, and they are also used in the parton shower.

The generating functional of the corresponding parton shower, which was described in [31] is given by

$$\mathcal{F}_n(t,O) \;=\; \sum_{l=n}^{\infty}\prod_{i=n+1}^{l}\left[\int_{t_c}^{t_{i-1}} \mathrm{d}\Phi_{1,i}\,\mathrm{K}_i(\Phi_{1,i})\,\Delta_{i-1}(t_i,t_{i-1})\right]\Delta_l(t_c,t_l)\,O(\Phi_l)\Big|_{t_n=t} \tag{7}$$

where K_l is the sum of evolution kernels for an l-parton state and Δ_n is the respective Sudakov factor. We define the parton-shower cutoff as t_c. This parton shower is based on the leading color approximation. It describes the QCD evolution of processes with only a single color configuration at leading order particularly well. Such reactions include the production of jets at e^+e^--colliders or the production of Drell–Yan lepton pairs at hadron colliders. Processes with a more complicated color structure at the leading order typically pose a problem for any type of parton shower, as the coherent emission of soft gluons can only be approximated by angular ordering [32, 33].

This problem is, to some extent, remedied by the implementation of the full-color MC@NLO technique as proposed in [27]. We exemplify the corresponding effects on physical observables in Fig. 1. The left panel shows that including full color coherence in the first emission has no substantial impact on observables like the transverse momentum of the $t\bar{t}$ pair. However, the right panel shows that it strongly affects the prediction for the p_T-dependent forward–backward asymmetry.

This effect is very different from a typical parton shower uncertainty. To exemplify this, we also show the effect of changing the scale at which the strong coupling is evaluated in the parton shower. Such a variation easily generates different transverse momentum spectra, but it does not affect the asymmetry, as can be seen by comparing the size of the red and blue bands in the left and right panels of Fig. 1. Both bands were generated by varying the scale in the range $\sqrt{1/2}\,k_T \ldots \sqrt{2}\,k_T$.

Similar statements hold for the choice of the momentum mapping, although they apply only within reason. Appendix A explains how the asymmetry is generated in a parton shower based on Catani-Seymour dipole factorization. If the assumption is relaxed that the recoil partner of the splitting parton is the color partner in the large-N_c limit, then the prediction for the asymmetry will change. This has already been demonstrated in [12] using the PYTHIA parton shower.

It should be stressed again that we only include the correct color insertion operators for the first emission, all subsequent branchings are generated in the standard shower approximation. Nevertheless, it is not unreasonable to assume that the overall picture remains for a complete full color evolution, as $p_{T,t\bar{t}}$ is largely generated by the first emission.

III. COMBINATION OF THE ZERO AND ONE JET PROCESS

Most practically implemented methods for combining matrix elements and parton showers are based on phase space slicing, with the soft part of the phase space populated by the parton shower, and the hard part populated by matrix elements, either at leading or at next-to-leading order. The slicing parameter is called the merging cut, Q_{cut}. It is given in a variable referred to as the jet criterion, Q.

The first working technique to achieve a combination of multiple NLO calculations for reactions at a hadron collider was introduced in [19]. It is based on the ideas of the CKKW [34, 35] and CKKW-L algorithms [36, 37]. We briefly review this method here to set the stage for a discussion of its uncertainties.

A. The MEPS@NLO method

In order to turn the inclusive parton-level calculations into exclusive n-jet predictions, which are to be combined, one needs to multiply them with no-emission probabilities, accounting for the fact that the inclusive cross section must be preserved at NLO.

The exclusive contribution to O from a parton-level calculation yielding n additional jets compared to the lowest multiplicity process reads [19]

$$\begin{aligned}\langle O\rangle_n^{\mathrm{excl}} \;=\; & \int \mathrm{d}\Phi_n\,\Theta(Q(\Phi_n)-Q_{\mathrm{cut}})\,\tilde{\mathrm{B}}_n^{(\mathrm{A})}(\Phi_n)\,\tilde{\mathcal{F}}_n^{(\mathrm{A})}(\mu_Q^2,O\,;{<}Q_{\mathrm{cut}}) \\ & + \int \mathrm{d}\Phi_{n+1}\,\Theta(Q(\Phi_n)-Q_{\mathrm{cut}})\,\Theta(Q_{\mathrm{cut}}-Q(\Phi_{n+1}))\,\tilde{\mathrm{H}}_n^{(\mathrm{A})}(\Phi_{n+1})\,\tilde{\mathcal{F}}_{n+1}(\mu_Q^2,O\,;{<}Q_{\mathrm{cut}})\;,\end{aligned} \tag{8}$$

where we have defined the generating functional of a truncated vetoed parton shower, $\tilde{\mathcal{F}}(<Q_{\mathrm{cut}})$. This parton shower may generate emissions at each point in a parton shower history which corresponds to the matrix-element configuration

at Φ_n.[2] We describe the respective evolution kernel by summing over all possible kernels for the intermediate steps:

$$\tilde{\mathrm{K}}_n(\Phi_{1,n+1}) \;=\; \mathrm{K}_n(\Phi_{1,n+1})\,\Theta(t_n - t_{n+1}) + \sum_{i=0}^{n-1} \mathrm{K}_i(\Phi_{1,n+1})\,\Theta(t_i - t_{n+1})\,\Theta(t_{n+1} - t_{i+1}) \Big|_{t_0=\mu_Q^2} . \tag{9}$$

One can now restrict emissions to the appropriate region of phase space by replacing $\mathrm{K}_i(\Phi_{1,n+1}) \to \mathrm{K}_i(\Phi_{1,n+1})\,\Theta(Q_{\mathrm{cut}} - Q(\Phi_i, \Phi_{1,n+1}))$. This implements the veto procedure. The corresponding generating functional of the truncated and vetoed parton shower is determined by substituting K with $\tilde{\mathrm{K}}$ in Eq. (7).

We have also defined modified NLO-weighted Born cross sections and hard remainder functions

$$\begin{aligned} \tilde{\mathrm{B}}_n^{(\mathrm{A})}(\Phi_n) \;&= \mathrm{B}_n(\Phi_n) + \tilde{\mathrm{V}}_n(\Phi_n) + \mathrm{I}_n^{(\mathrm{S})}(\Phi_n) + \int \mathrm{d}\Phi_1 \,\left[\tilde{\mathrm{D}}_n^{(\mathrm{A})}(\Phi_n, \Phi_1) - \mathrm{D}_n^{(\mathrm{S})}(\Phi_n, \Phi_1)\right] \\ \tilde{\mathrm{H}}_n^{(\mathrm{A})}(\Phi_{n+1}) \;&= \mathrm{R}_n(\Phi_{n+1}) - \tilde{\mathrm{D}}_n^{(\mathrm{A})}(\Phi_{n+1}) \end{aligned} \tag{10}$$

which are given in terms of the compound evolution kernel $\tilde{\mathrm{D}}_n^{(\mathrm{A})}$,

$$\tilde{\mathrm{D}}_n^{(\mathrm{A})}(\Phi_{n+1}) \;=\; \mathrm{D}_n^{(\mathrm{A})}(\Phi_{n+1})\,\Theta(t_n - t_{n+1}) \;+ \sum_{i=0}^{n-1} \mathrm{B}_n(\Phi_n)\,\mathrm{K}_i(\Phi_{1,n+1})\,\Theta(t_i - t_{n+1})\,\Theta(t_{n+1} - t_{i+1}) \Big|_{t_0=\mu_Q^2} . \tag{11}$$

The first term on the right-hand side of Eq. (11) resembles the resummed part of the real-emission correction in the original MC@NLO (cf. Eq. (2)), while the second term is identical to the one in Eq. (9). It is mandatory to implement color coherence in the first term, while it is optional in the second term, since the evolution variable is bounded from below by t_n. One finally obtains the generating functional for the combined truncated vetoed parton shower plus MC@NLO, $\tilde{\mathcal{F}}^{(\mathrm{A})}(<Q_{\mathrm{cut}})$, by replacing the evolution kernel for the first step in $\tilde{\mathcal{F}}(<Q_{\mathrm{cut}})$ with the compound kernel in Eq. (11).

While the structure of Eqs. (8)-(11) seems quite involved, their interpretation is rather simple: MC@NLO itself is a modified subtraction method, which allows to correct for the mismatch between the parton shower approximation and the full NLO calculation in the first emission step. As we encounter processes where truncated parton showers can generate emissions, we have to take these emissions into account in the modified subtraction. This leads to the definition of Eq. (10) and the compound evolution kernel, Eq. (11).

B. Theoretical uncertainties

The uncertainties associated with the above defined MEPS@NLO method fall into three categories: The first are uncertainties related to the choice of renormalization and factorization scale. They occur in every NLO calculation. The second are uncertainties due to the choice of parton shower parameters, which occur in every parton shower simulation. A typical example is the choice of resummation scale, μ_Q^2. The last, and final uncertainty is related to the choice of the merging cut, Q_{cut}, and the choice of the functional form of jet criterion.[3] We find that the variation associated with the choice of resummation scale is in most cases smaller than the statistical uncertainty in our simulation. The other two types of uncertainties are discussed in the following.

Merging uncertainties

The left panel of Fig. 2 displays the effect of varying Q_{cut} in the range from 5 to 10 GeV. Effects on the $\log p_{T,t\bar{t}}$ spectrum are below 10%. Potential discontinuities in the transition from the zero to the one jet domain are generated by differences between the $t\bar{t}$ MC@NLO at finite transverse momentum and the $t\bar{t}$+jet MC@NLO. Out of the two predictions, the $t\bar{t}$ MC@NLO is less accurate. Small discontinuities therefore indicate that it still provides a good estimate of the $t\bar{t}$+jet production rate at NLO. This means that we can reliably compute the transverse momentum dependent asymmetry, except for the first bin, where the prediction is formally still only LO accurate due to the large contribution from the $t\bar{t}$ MC@NLO.

---

[2] A detailed algorithm for identifying these parton shower histories is discussed in [35, 36].

[3] Strictly speaking this is not an uncertainty, as one would attempt to choose the parameters such that the phase-space region of interest for experimental analyses is always fully covered by respective NLO parton-level calculations [34].

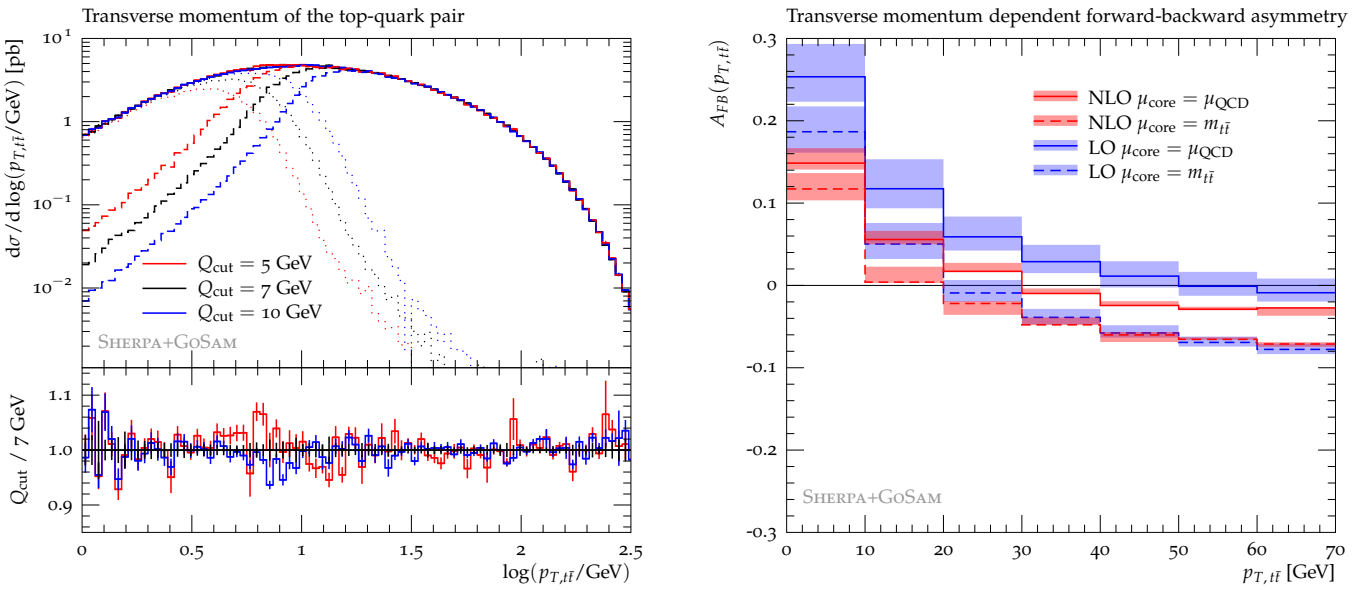

FIG. 2. Systematic uncertainty due to variation of the merging cut (left) and due to the scale choice (right). The dotted (dashed) lines in the left panel correspond to contributions from the zero (one) jet MC@NLO. The two bands in the right panel depict results from different choices of the functional form of the core scale, for more details see the main text. Each band has been obtained by varying the respective default scale by factors of two.

Note that we observe unitarity violations in our merging approach. A comprehensive analysis of the unitarity constraint on the parton shower in the context of merging algorithms was presented recently [38], and a new method has been proposed to restore the overall normalization of the inclusive event sample exactly [37]. Here, we follow a simpler approach, where unitarity violations may occur, but their impact on the total cross section is beyond the order at which we claim our calculation to be exact [19].

Scale uncertainties

The right panel of Fig. 2 displays the uncertainty arising from a variation of renormalization and factorization scales in the range $1/2\,\mu_{R/F} \ldots 2\,\mu_{R/F}$. The two different bands were generated by choosing the central scale for the $p\bar{p} \to t\bar{t}$ "core" process in the simulation as either the invariant mass of the $t\bar{t}$-system, or as twice the product of four-momenta of the color-connected partons in the large-N_c limit of the "core" process. We will refer to the latter scale choice as the "QCD" scale. It is described in detail in Appendix C.

Fig. 2 shows that both, the variation of the scale prefactor (leading to the uncertainty bands) and the variation of the functional form of the core scale (leading to the solid/dashed central histograms) have less impact on the predictions from the MEPS@NLO method than they have on predictions from leading–order merging (MEPS@LO). It is interesting to find this effect in an observable like the forward–backward asymmetry, where a large fraction of the QCD uncertainties are canceled due to taking the ratio between two predictions.

IV. A_{FB} RESULTS

We now present our A_{FB} results generated with the previously described techniques. We employ the leading-order matrix element generators AMEGIC++ [39] and COMIX [40] in conjunction with the automated dipole subtraction provided in SHERPA [41] and the implementation of the Binoth–Les Houches interface [26] to obtain parton-level events at next-to-leading order. Virtual matrix elements for $t\bar{t}$ and $t\bar{t}$+jet are provided by GOSAM [21]. We use a parton shower based on Catani–Seymour dipole factorization [31, 42] and the related MC@NLO generator [27, 43] to generate events at the parton shower level.

We use SHERPA version 2.0.0, which includes the modifications described in Sec. II. Parameters are set to their default values, except for the choice of PDF. We use the MSTW2008 NLO PDF set for MEPS@NLO and the MSTW2008 LO set for MEPS@LO, both with their corresponding parametrization of the strong coupling [44]. Top quark decays,

Source	$A_{\rm FB}$ [%]	$A_{\rm FB}(m_{t\bar{t}})$ [%]		$A_{\rm FB}(p_{T,t\bar{t}})$ [%]	
	inclusive	$m < 450\,\text{GeV}$	$m > 450\,\text{GeV}$	$p_T < 50\,\text{GeV}$	$p_T > 50\,\text{GeV}$
PRD**87** (2013) 092002	16.4 ± 4.7	8.4 ± 5.5	29.5 ± 6.7	–	–
MEPS@NLO, $\mu = \mu_{\rm QCD}$	$8.5\,^{+0.5}_{-0.5}$	$6.1\,^{+0.2}_{-0.1}$	$12.7\,^{+1.1}_{-0.6}$	$9.5\,^{+0.7}_{-0.0}$	$-3.4\,^{-0.8}_{-0.1}$
MEPS@NLO, $\mu = m_{t\bar{t}}$	$4.8\,^{+0.7}_{-0.3}$	$3.1\,^{+0.8}_{+0.1}$	$7.9\,^{+0.5}_{-1.1}$	$5.8\,^{+0.8}_{-0.4}$	$-7.2\,^{+0.5}_{-0.4}$
MEPS@LO, $\mu = \mu_{\rm QCD}$	$15.0\,^{+1.9}_{-1.4}$	$11.0\,^{+1.4}_{-1.1}$	$22.2\,^{+2.3}_{-2.0}$	$16.6\,^{+2.2}_{-1.6}$	$-1.1\,^{+1.7}_{-1.2}$
MEPS@LO, $\mu = m_{t\bar{t}}$	$8.2\,^{+0.9}_{-0.8}$	$5.9\,^{+0.6}_{-0.6}$	$12.5\,^{+1.3}_{-1.2}$	$9.9\,^{+1.1}_{-1.1}$	$-7.9\,^{+0.6}_{-0.6}$
NLO $p\bar{p} \to t\bar{t}$	6.0	4.1	9.3	7.0	-11.1

TABLE I. Top quark forward–backward asymmetry at the parton level. We compare experimental data from CDF [5], results from an NLO parton-level $p\bar{p} \to t\bar{t}$ calculation obtained with MCFM [4, 10] (last row) and predictions in the NLO and LO merging schemes from SHERPA. The set of uncertainties next to all SHERPA predictions has been determined by varying renormalization and factorization scales in the range from 1/2 (upper) to 2 (lower). We give predictions at the parton level for both of the central scale choices discussed in Sec. III B.

multiple interactions and hadronization are not simulated, since we compare our results to data from the CDF collaboration which have been corrected to the parton level.

We have validated our parton-level calculations by checking inclusive cross sections for $t\bar{t}$+jets against values in the literature [3]. Tests for individual phase-space points are reported in Appendix B. We also verified the consistency of our results for a number of differential distributions in inclusive $t\bar{t}$ production.

A. Inclusive asymmetries

Table I lists the inclusive forward–backward asymmetry, as well as the asymmetries arising after simple cuts on the invariant mass of the top-quark pair and its transverse momentum. These cuts separate the threshold and boosted region in the case of $m_{t\bar{t}}$, and the Sudakov and hard-p_T region in the case of $p_{T,t\bar{t}}$. We present results for both the MEPS@NLO and the MEPS@LO methods and compare them to data from the CDF collaboration [5], and to a fixed-order calculation for the asymmetry evaluated at scale $\hat{s}$ using MCFM [4, 10].

The largest contribution to the overall uncertainty of our predictions arises from $\mu_{\rm R/F}$ variation – those from other sources are by and large negligible. We observe a sizable reduction of scale uncertainties when going from LO to NLO merging, which was already noted in Sec. III B. At the same time, however, the central values of $A_{\rm FB}$ decrease and therefore the discrepancy with the CDF data increases. It should be stressed that the MEPS@LO results for $A_{\rm FB}$ have to be interpreted with caution. The lack of important higher-order corrections in their calculation, and the correspondingly large scale uncertainties, point to an agreement with experimental data that is rather accidental. Signs of an incomplete, only qualitative description are also given by the larger spread between the central values associated with the different functional forms of the core scale. Moreover, the discrepancy, in particular for the lowest p_T bin in $A_{\rm FB}(p_{T,t\bar{t}})$ poses a problem, as can be seen in Fig. 2.

The disentanglement of the soft and hard regime can be easily achieved in terms of $p_{T,t\bar{t}}$. It would therefore be interesting to obtain independent measurements for the two different transverse momentum regions, preferably for an even lower cut. Due to the formal NLO accuracy of the MEPS@NLO result for $p_{T,t\bar{t}} > 50\,\text{GeV}$ we expect a better agreement with data. This is in fact confirmed in Fig. 3

B. Differential asymmetries

Figure 3 summarizes our results for the differential asymmetries. We compare our best predictions, those obtained with MEPS@NLO, against the measured distributions for $A_{\rm FB}$ in dependence on the pair transverse momentum, the pair mass and the absolute rapidity difference between the top quarks. For all predictions, we show uncertainty bands, which have been obtained from respectively varying $\mu_{\rm R/F}$ and μ_Q scales by factors of two and $\sqrt{2}$, and the merging cut, $Q_{\rm cut}$, from 5 GeV to 10 GeV where we used $Q_{\rm cut} = 7\,\text{GeV}$ for the central curve. The individual uncertainties are added in quadrature. They are dominated by the $\mu_{\rm R/F}$ variations. Parton-level to particle-level corrections for

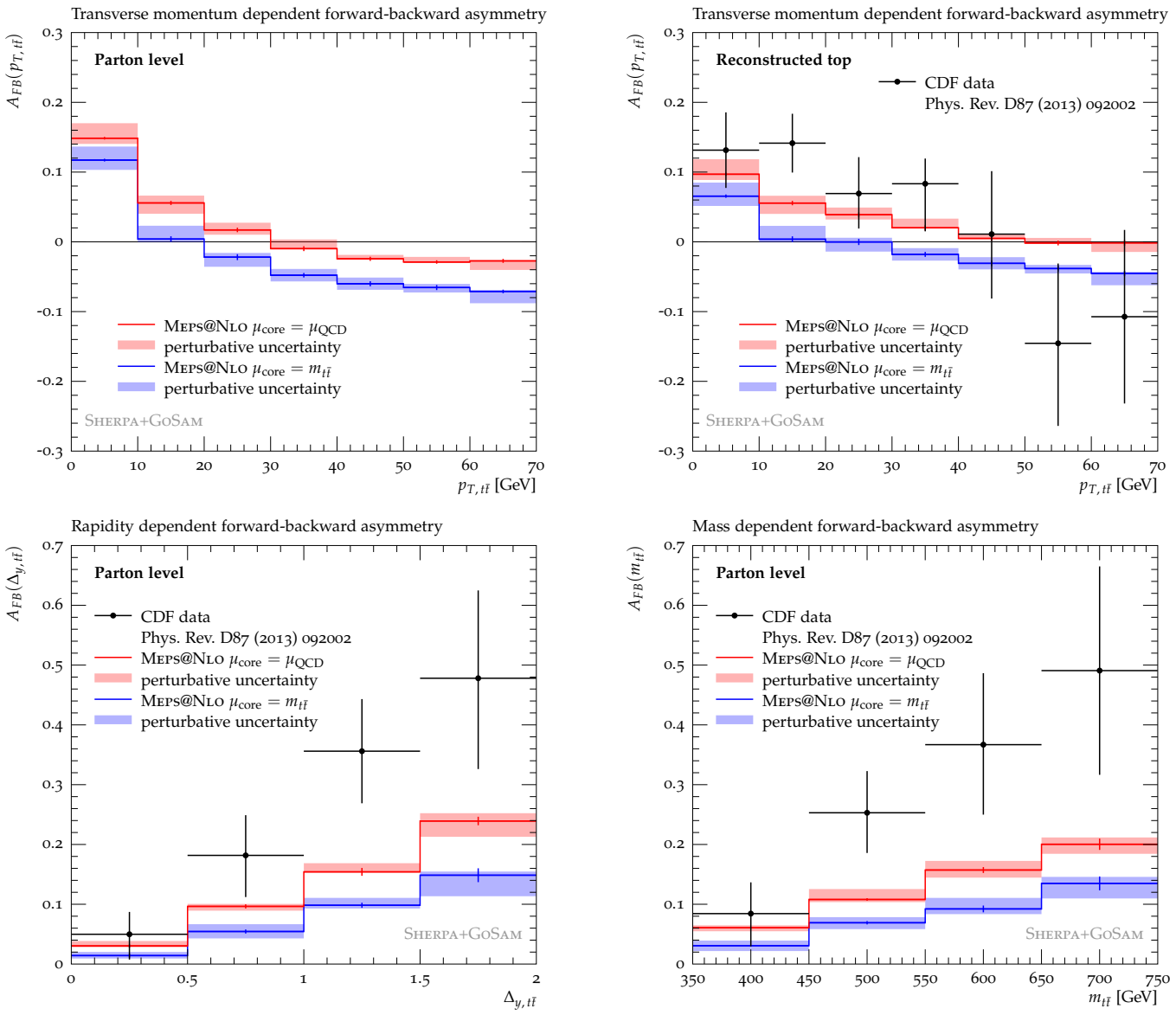

FIG. 3. Top quark forward–backward asymmetry in dependence on the transverse momentum (top), the absolute of the rapidity separation, $\Delta_{y,t\bar{t}} \equiv |y_t - y_{\bar{t}}|$ (bottom left), and the invariant mass (bottom right) of the $t\bar{t}$ system. MC@NLO zero plus one jet merged predictions – together with their uncertainty bands – are shown for both of the scale choices studied in this work, cf. Sec. III B. The comparison is against CDF background subtracted data (top right panel) and against parton-level corrected data (bottom panels) [5]. The top left panel shows parton-level results.

the comparison with the background subtracted data on $A_{\rm FB}(p_{T,t\bar{t}})$ have been computed with SHERPA in MC@NLO mode.

We find good agreement with the CDF data for $A_{\rm FB}(p_{T,t\bar{t}})$. This is an important result, since we obtain this quantitative agreement in two very different phase-space domains driven by different physics phenomena: multiple soft and virtual parton emission in the so-called Sudakov region and hard parton radiation for larger pair transverse momenta. The prediction based on the QCD scale choice, which we discussed in Sec. III B, gives a slightly better description in the medium pair-p_T range. In both cases we observe excellent agreement in the first p_T bin, as a result of relying on the subleading-color improved MC@NLO Sudakov exponents.

In the other two observables considered here, the Sudakov region is spread out over the entire range of the measurement. This leads to an increase of $A_{\rm FB}$ for larger values of $m_{t\bar{t}}$ and $\Delta_{y,t\bar{t}}$. Both core scale choices, $\mu_{\rm QCD}$ and $m_{t\bar{t}}$, yield predictions, which reproduce the linear rise but remain below the data. Once more, the results obtained using the QCD scale lie closer to the data, and well in the $2\,\sigma$ range of the given experimental uncertainty. Note that

the asymmetry dependence on these observables will particularly benefit from the application of $\mathcal{O}(25\%)$ electroweak corrections, which have not yet been included in Fig. 3.

V. CONCLUSIONS

We have analyzed the top quark forward–backward asymmetry at the Tevatron collider using a combination of $t\bar{t}$ and $t\bar{t}$+jet calculations at the next-to-leading order in QCD, merged with a parton shower.

The asymmetry as measured by the CDF and DØ collaborations still remains a puzzle. While our simulations describe its transverse momentum dependence well, the rapidity and mass dependence still show some discrepancies. More accurate QCD+EW predictions are paramount to clarify whether what was measured can be described within the Standard Model, or whether new physics models are needed. There is also hope that measurements at the LHC may bring some more insight, although the current situation still suffers from a lack of analyzed data [45].

However, a number of interesting points remain: firstly, we have achieved a consistent description of both, the Sudakov region of the $p_{T,t\bar{t}}$ spectrum and the high $p_{T,t\bar{t}}$ domain. The transverse momentum dependent forward–backward asymmetry provides a first non-trivial test of this method. The fact that it is well described by our simulations indicates the potential of the MEPS@NLO technique. Secondly, we demonstrated in a thorough analysis that the application of the MEPS@NLO technique leads to more stable predictions than the MEPS@LO method. It should thus be preferred in experimental analyses. Thirdly, we showed that including subleading color terms in the first emission of the $t\bar{t}$ MC@NLO has substantial impact on the prediction for the asymmetry. This effect cannot simply be subsumed under the standard parton-shower uncertainties. The fact that the difference between MC@NLO and MEPS@NLO predictions is small indicates that the feature remains in a parton shower with full color dependence. Fourthly, we showed that there is a substantial dependence on the functional form of the scale, which is used for the $t\bar{t}$ production process. This dependence is reduced in the MEPS@NLO method compared to the MEPS@LO method, but it indicates that there is still room for explaining the discrepancy with experiments by QCD+EW corrections at higher orders.

In summary, we have moved one step closer to obtaining an accurate inclusive prediction for top-quark pair production at the particle level using state-of-the-art Monte Carlo techniques. We used the publicly available programs SHERPA and GOSAM, which makes the results easily reproduceable and accessible for experiments.

We have performed our calculations at the parton shower level, not including top-quark decays. Including these decays is important to predict lepton asymmetries and their correlation with the top quark asymmetry more reliably, see for example Refs. [46]. This analysis is beyond the scope of the present publication, and it will be left to future investigation.

ACKNOWLEDGEMENTS

We are indebted to Lance Dixon, Ye Li and Huaxing Zhu for many fruitful discussions. We thank Francesco Tramontano for help with technical aspects of GOSAM. SH's and JH's work was supported by the U.S. Department of Energy under Contract No. DE–AC02–76SF00515. MS's work was supported by the Research Executive Agency (REA) of the European Union under the Grant Agreement number PITN-GA-2010-264564 (LHCPhenoNet). GL, MS and JW thank the organizers of the Les Houches 2013 workshop "Physics at TeV Colliders" for providing a stimulating atmosphere during the final stages of this project. The work of GL was supported by the Alexander von Humboldt Foundation, in the framework of the Sofja Kovaleskaja Award Project "Advanced Mathematical Methods for Particle Physics", endowed by the German Federal Ministry of Education and Research. This research used the CERN computing facilities, the National Energy Research Scientific Computing Center, which is supported by the Office of Science of the U.S. Department of Energy under Contract No. DE–AC02–05CH11231, and resources provided by the Open Science Grid, which is supported by the National Science Foundation and the U.S. Department of Energy.

Appendix A: IF/FI dipole splitting kinematics and their implications on A_{FB}

In this appendix we will prove that for a parton shower based on CDST dipole factorization [31] P_{-+} is larger than P_{+-}, as found by numerical analysis in [12].

Let us start with the case of initial-state splittings, where the top quark plays the role of the spectator parton. Denoting the initial and final state momenta before the splitting as $\tilde{p}_{ai}$ and $\tilde{p}_k$, we can construct the momentum of

the top quark after splitting using the variables u_i and $x_{ik,a}$ of [30] as

$$p_k \;=\; (1-u_i)\,\tilde{p}_k + u_i\left(\frac{1-x_{ik,a}}{x_{ik,a}} - \frac{2m_k^2}{Q^2-m_k^2}\right)\tilde{p}_{ai} - k_\perp\;, \tag{A1}$$

where $k_\perp$ is the transverse component, perpendicular to both, $\tilde{p}_k$ and $\tilde{p}_{ai}$. This means, in particular, that $k_\perp$ can be neglected when analyzing the change of rapidity of the top quark in the splitting process.

We can now easily compute the rapidity difference for the top quark before and after the splitting:

$$\Delta y_t \;=\; \frac{1}{2}\ln\left(1+\frac{u_i}{1-u_i}\left(\frac{1-x_{ik,a}}{x_{ik,a}} - \frac{2m_k^2}{Q^2-m_k^2}\right)\frac{\tilde{p}_{ai}^{\,+}}{\tilde{p}_k^{\,+}}\right) \tag{A2}$$

As $Q^2 < 0$, the argument of the logarithm is always larger than one, and therefore Δy_t is positive. This means the top quark is always pushed in the direction of the momentum of the initial-state quark while the anti-top is pushed in the direction of the momentum of the initial-state anti-quark. The same is true for the case of final-state emissions off the top quark with an initial-state spectator, as kinematics are defined identically.

At the Tevatron collider, the dominant source of quarks is the proton beam, while the dominant source of antiquarks is the anti-proton beam. Therefore, the initial-final and final-initial splittings lead to $P_{-+} > P_{+-}$.

Final-state splittings with final-state spectator and initial-state splittings with initial-state spectator do not generate asymmetries, i.e. $P_{-+} = P_{+-}$. Therefore, our argument is complete.

Note that the two different schemes for momentum mapping, which were compared in [42, 47], have similar behavior with respect to the generation of the asymmetry. This was shown in a detailed numerical analysis in [12]. It can easily be explained by the fact that both schemes show a drag of the top towards larger rapidity due to the color connection with the initial-state quark.

It was also shown in [12] that a very different momentum mapping can generate very different asymmetry predictions. This is due to the fact that assumptions about the recoil partner being the color-connected parton in the splitting were relaxed. It is conceivable that, in a momentum mapping where the recoil is compensated symmetrically by both initial state quarks, the parton shower does not generate an additional asymmetry at all. Whether or not this is the more viable physics model remains to be verified by experiments.

Appendix B: Virtual corrections from GoSam

The virtual amplitudes are generated using the GoSam [21] package, which generates code for the computation of one-loop integrands. The one-loop amplitudes are then evaluated at runtime by means of the integrand reduction [23] based program Samurai [22] and the tensor integral library Golem95 [24]. Scalar one-loop integrals are calculated by OneLOop [48].

We validated the virtual amplitudes from GoSam with the benchmark points given in [3], finding full agreement. Since we use a different normalization compared to [3] we define coefficients $\tilde{c}_i$ ($i = -2, -1, 0$) from the coefficients c_i given in Eq. (A.3) of [3] as follows:

$$\tilde{c}_{-2} = \frac{c_{-2}}{\frac{\alpha_s}{2\pi}}, \qquad \tilde{c}_{-1} = \frac{c_{-1}}{\frac{\alpha_s}{2\pi}}, \qquad \tilde{c}_0 = \frac{c_0}{\frac{\alpha_s}{2\pi}} + \frac{\pi^2}{6}\tilde{c}_{-2} \qquad \text{with} \quad \alpha_s \equiv \alpha_s(m_t) = 0.1075205492734706\,. \tag{B1}$$

In Tab. II we then report the details of the comparison listing all Born numbers and coefficients, which we found in our calculation.

Appendix C: Color-flow inspired scale choice

In order to quantify the dependence of A_{FB} on renormalization and factorization scales, we propose to use two different functional forms of the scale, where one is insensitive and the other is sensitive to rapidity. For the former, we select $m_{t\bar{t}}$, while for the latter we select a color-flow inspired scale. We call this the "QCD" scale for brevity.

The color flow in $q\bar{q} \to t\bar{t}$ / $\bar{q}q \to t\bar{t}$ subprocesses is unique, hence the QCD scale is identified as

$$\begin{aligned}\mu^2_{\text{QCD}}(q\bar{q} \to t\bar{t}) &= 2\,p_q p_t = m_t^2 - t\;,\\ \mu^2_{\text{QCD}}(\bar{q}q \to t\bar{t}) &= 2\,p_q p_t = m_t^2 - u\;.\end{aligned} \tag{C1}$$

$d\bar{d} \to t\bar{t}g$			
	SHERPA + GOSAM	Numbers from [3]	Universal IR singularity
Born	$0.5790368001550917 \cdot 10^{-4}$	$0.5790368001550936 \cdot 10^{-4}$	
$\tilde{c}_{-2}$	-5.666666666666674	-5.666666666667982	-5.666666666666667
$\tilde{c}_{-1}$	-0.7420525970833627	-0.7420525970851204	-0.7420525970837827
$\tilde{c}_0$	4.912061786537501	4.912061774385727	
c_0	0.2435672441163395	0.2435672439083931	

$gg \to t\bar{t}g$			
	SHERPA + GOSAM	Numbers from [3]	Universal IR singularity
Born	$0.656684336270973 \cdot 10^{-3}$	$0.656684336270977 \cdot 10^{-3}$	
$\tilde{c}_{-2}$	-8.999999999999995	-8.999999999455426	-9.000000000000002
$\tilde{c}_{-1}$	4.272315663799295	4.272315664361962	4.272315663817603
$\tilde{c}_0$	16.13909120795238	16.13909126125360	
c_0	0.5295183443224957	0.5295183452346090	

TABLE II. Numerical results for the benchmark-point comparison with [3]. The first column contains the numbers obtained with the code for the virtual amplitude generated by GOSAM. In the second column we report the numbers given in [3] converted to our normalization. The last column contains the coefficients of the poles conform to the universal singular behavior derived by CDST [30]. They are computed using an implementation contained in the code for virtual amplitudes.

In the $gg \to t\bar{t}$ subprocess we assign color connections according to the method used in [33], extended to the case with massive final-state quarks. The QCD scale is therefore chosen as

$$\mu^2_{\mathrm{QCD}}(gg \to t\bar{t}) = \begin{cases} m_t^2 - t & w \propto \dfrac{u-m_t^2}{t-m_t^2} + \dfrac{m_t^2}{m_t^2-t}\left(\dfrac{4\,t}{t-m_t^2} + \dfrac{m_t^2}{s}\right) \\ \text{with weight} & \\ m_t^2 - u & w \propto \dfrac{t-m_t^2}{u-m_t^2} + \dfrac{m_t^2}{m_t^2-u}\left(\dfrac{4\,u}{u-m_t^2} + \dfrac{m_t^2}{s}\right) \end{cases} . \tag{C2}$$

Because of the symmetric initial state, $m_t^2 - t$ and $m_t^2 - u$ are selected with equal probability.

[1] V. Abazov et al., The DØ collaboration, *First measurement of the forward-backward charge asymmetry in top quark pair production*, Phys.Rev.Lett. **100** (2008), 142002, [arXiv:0712.0851 [hep-ex]]; T. Aaltonen et al., The CDF collaboration, *Forward-Backward Asymmetry in Top Quark Production in $p\bar{p}$ Collisions at $\sqrt{s} = 1.96$ TeV*, Phys.Rev.Lett. **101** (2008), 202001, [arXiv:0806.2472 [hep-ex]]; T. Aaltonen et al., The CDF collaboration, *Evidence for a Mass Dependent Forward-Backward Asymmetry in Top Quark Pair Production*, Phys.Rev. **D83** (2011), 112003, [arXiv:1101.0034 [hep-ex]]; V. M. Abazov et al., The DØ collaboration, *Forward-backward asymmetry in top quark-antiquark production*, Phys.Rev. **D84** (2011), 112005, [arXiv:1107.4995 [hep-ex]].

[2] J. H. Kuhn and G. Rodrigo, *Charge asymmetry of heavy quarks at hadron colliders*, Phys.Rev. **D59** (1999), 054017, [arXiv:hep-ph/9807420 [hep-ph]]; O. Antunano, J. H. Kühn and G. Rodrigo, *Top Quarks, Axigluons and Charge Asymmetries at Hadron Colliders*, Phys. Rev. **D77** (2008), 014003, [arXiv:0709.1652 [hep-ph]]; L. G. Almeida, G. F. Sterman and W. Vogelsang, *Threshold Resummation for the Top Quark Charge Asymmetry*, Phys.Rev. **D78** (2008), 014008, [arXiv:0805.1885 [hep-ph]]; N. Kidonakis, *The top quark rapidity distribution and forward-backward asymmetry*, Phys.Rev. **D84** (2011), 011504, [arXiv:1105.5167 [hep-ph]]; V. Ahrens, A. Ferroglia, M. Neubert, B. D. Pecjak and L. L. Yang, *The top-pair forward-backward asymmetry beyond NLO*, Phys.Rev. **D84** (2011), 074004, [arXiv:1106.6051 [hep-ph]]; J. H. Kühn and G. Rodrigo, *Charge asymmetries of top quarks at hadron colliders revisited*, JHEP **1201** (2012), 063, [arXiv:1109.6830 [hep-ph]]; S. Alioli, S.-O. Moch and P. Uwer, *Hadronic top-quark pair-production with one jet and parton showering*, JHEP **1201** (2012), 137, [arXiv:1110.5251 [hep-ph]]; K. Melnikov, A. Scharf and M. Schulze, *Top quark pair production in association with a jet: QCD corrections and jet radiation in top quark decays*, Phys.Rev. **D85** (2012), 054002, [arXiv:1111.4991 [hep-ph]]; A. V. Manohar and M. Trott, *Electroweak Sudakov Corrections and the Top Quark Forward-Backward Asymmetry*, Phys.Lett. **B711** (2012), 313–316, [arXiv:1201.3926 [hep-ph]]; S. J. Brodsky and X.-G. Wu, *Application of the Principle of Maximum Conformality to the Top-Quark Forward-Backward Asymmetry at the Tevatron*, Phys.Rev. **D85** (2012), 114040, [arXiv:1205.1232 [hep-ph]].

[3] S. Dittmaier, P. Uwer and S. Weinzierl, *Hadronic top-quark pair production in association with a hard jet at next-to-leading*

order QCD: Phenomenological studies for the Tevatron and the LHC, Eur.Phys.J. **C59** (2009), 625–646, [arXiv:0810.0452 [hep-ph]].

[4] J. M. Campbell and R. K. Ellis, *Top-quark processes at NLO in production and decay*, arXiv:1204.1513 [hep-ph].

[5] T. Aaltonen et al., The CDF collaboration, *Measurement of the top quark forward-backward production asymmetry and its dependence on event kinematic properties*, Phys.Rev. **D87** (2013), 092002, [arXiv:1211.1003 [hep-ex]].

[6] S. Frixione and B. R. Webber, *Matching NLO QCD computations and parton shower simulations*, JHEP **06** (2002), 029, [hep-ph/0204244].

[7] S. Frixione, P. Nason and B. R. Webber, *Matching NLO QCD and parton showers in heavy flavour production*, JHEP **08** (2003), 007, [hep-ph/0305252].

[8] P. Nason, *A new method for combining NLO QCD with shower Monte Carlo algorithms*, JHEP **11** (2004), 040, [hep-ph/0409146]; S. Frixione, P. Nason and C. Oleari, *Matching NLO QCD computations with parton shower simulations: the POWHEG method*, JHEP **11** (2007), 070, [arXiv:0709.2092 [hep-ph]]; S. Alioli, P. Nason, C. Oleari and E. Re, *A general framework for implementing NLO calculations in shower Monte Carlo programs: the POWHEG BOX*, JHEP **06** (2010), 043, [arXiv:1002.2581 [hep-ph]]; S. Höche, F. Krauss, M. Schönherr and F. Siegert, *Automating the POWHEG method in Sherpa*, JHEP **04** (2011), 024, [arXiv:1008.5399 [hep-ph]].

[9] S. Frixione, P. Nason and G. Ridolfi, *A positive-weight next-to-leading-order Monte Carlo for heavy flavour hadroproduction*, JHEP **09** (2007), 126, [arXiv:0707.3088 [hep-ph]].

[10] J. M. Campbell and R. Ellis, *MCFM for the Tevatron and the LHC*, Nucl.Phys.Proc.Suppl. **205-206** (2010), 10–15, [arXiv:1007.3492 [hep-ph]].

[11] P. H. Frampton and S. L. Glashow, *Chiral Color: An Alternative to the Standard Model*, Phys. Lett. **B190** (1987), 157; K. Agashe, A. Belyaev, T. Krupovnickas, G. Perez and J. Virzi, *LHC signals from warped extra dimensions*, Phys. Rev. **D77** (2008), 015003, [hep-ph/0612015]; V. Barger, T. Han and D. G. Walker, *Top Quark Pairs at High Invariant Mass: A Model-Independent Discriminator of New Physics at the LHC*, Phys.Rev.Lett. **100** (2008), 031801, [arXiv:hep-ph/0612016 [hep-ph]]; R. Frederix and F. Maltoni, *Top pair invariant mass distribution: A Window on new physics*, JHEP **0901** (2009), 047, [arXiv:0712.2355 [hep-ph]]; A. Djouadi, G. Moreau, F. Richard and R. K. Singh, *The Forward-backward asymmetry of top quark production at the Tevatron in warped extra dimensional models*, Phys.Rev. **D82** (2010), 071702, [arXiv:0906.0604 [hep-ph]]; M. Bauer, F. Görtz, U. Haisch, T. Pfoh and S. Westhoff, *Top-Quark Forward-Backward Asymmetry in Randall-Sundrum Models Beyond the Leading Order*, JHEP **1011** (2010), 039, [arXiv:1008.0742 [hep-ph]]; D. Choudhury, R. M. Godbole, S. D. Rindani and P. Saha, *Top polarization, forward-backward asymmetry and new physics*, Phys.Rev. **D84** (2011), 014023, [arXiv:1012.4750 [hep-ph]]; J. Cao, L. Wu and J. M. Yang, *New physics effects on top quark spin correlation and polarization at the LHC: a comparative study in different models*, Phys.Rev. **D83** (2011), 034024, [arXiv:1011.5564 [hep-ph]]; R. Barcelo, A. Carmona, M. Masip and J. Santiago, *Gluon excitations in $t\bar{t}$ production at hadron colliders*, Phys.Rev. **D84** (2011), 014024, [arXiv:1105.3333 [hep-ph]]; R. Barcelo, A. Carmona, M. Masip and J. Santiago, *Stealth gluons at hadron colliders*, Phys.Lett. **B707** (2012), 88–91, [arXiv:1106.4054 [hep-ph]]; J. F. Kamenik, J. Shu and J. Zupan, *Review of New Physics Effects in $t\bar{t}$ Production*, Eur.Phys.J. **C72** (2012), 2102, [arXiv:1107.5257 [hep-ph]]; J. Aguilar-Saavedra and M. Perez-Victoria, *Shaping the top asymmetry*, Phys.Lett. **B705** (2011), 228–234, [arXiv:1107.2120 [hep-ph]]; G. Marques Tavares and M. Schmaltz, *Explaining the $t\bar{t}$ asymmetry with a light axigluon*, Phys.Rev. **D84** (2011), 054008, [arXiv:1107.0978 [hep-ph]]; E. L. Berger, Q.-H. Cao, C.-R. Chen and H. Zhang, *Top Quark Polarization As A Probe of Models with Extra Gauge Bosons*, Phys.Rev. **D83** (2011), 114026, [arXiv:1103.3274 [hep-ph]]; V. Barger, W.-Y. Keung and C.-T. Yu, *Looking for parity nonconservation from strong interactions beyond QCD*, Phys.Rev. **D85** (2012), 056008, [arXiv:1108.2275 [hep-ph]]; Y. Bai, J. L. Hewett, J. Kaplan and T. G. Rizzo, *LHC Predictions from a Tevatron Anomaly in the Top Quark Forward-Backward Asymmetry*, JHEP **1103** (2011), 003, [arXiv:1101.5203 [hep-ph]]; J. Aguilar-Saavedra and A. Juste, *Collider-independent $t\bar{t}$ forward-backward asymmetries*, Phys.Rev.Lett. **109** (2012), 211804, [arXiv:1205.1898 [hep-ph]]; E. Alvarez and E. C. Leskow, *A charged Z' to conciliate the apparent disagreement between top-antitop Tevatron forward-backward asymmetry and LHC charge asymmetry*, Phys.Rev. **D86** (2012), 114034, [arXiv:1209.4354 [hep-ph]]; J. Drobnak, J. F. Kamenik and J. Zupan, *Flipping $t\bar{t}$ asymmetries at the Tevatron and the LHC*, arXiv:1205.4721 [hep-ph]; J. Drobnak, A. L. Kagan, J. F. Kamenik, G. Perez and J. Zupan, *Forward Tevatron Tops and Backward LHC Tops with Associates*, arXiv:1209.4872 [hep-ph]; L. Da Rold, C. Delaunay, C. Grojean and G. Perez, *Up Asymmetries From Exhilarated Composite Flavor Structures*, arXiv:1208.1499 [hep-ph]; C. Han, N. Liu, L. Wu, J. M. Yang and Y. Zhang, *Two-Higgs-doublet model with a color-triplet scalar: a joint explanation for top quark forward-backward asymmetry and Higgs decay to diphoton*, arXiv:1212.6728 [hep-ph]; D. Palle, *On the anomalous t-quark charge asymmetry and noncontractibility of the physical space*, Acta Phys.Pol. **B43** (2012), 2055, [arXiv:1204.1171 [physics.gen-ph]]; W.-C. Huang and A. Urbano, *What the top asymmetries tell us about single top production and Higgs decays*, JHEP **1303** (2013), 079, [arXiv:1212.1399 [hep-ph]]; M. Baumgart and B. Tweedie, *Transverse Top Quark Polarization and the ttbar Forward-Backward Asymmetry*, arXiv:1303.1200 [hep-ph]; C. Li, C.-D. Lu and X.-D. Gao, *Study the Forward-Backward Asymmetry of the Top Quark Production in the Randall-Sundrum Model with an Extension of Strong Interaction*, arXiv:1303.5646 [hep-ph]; R. S. Chivukula, E. H. Simmons and N. Vignaroli, *A Flavorful Top-Coloron Model*, Phys.Rev. **D87** (2013), 075002, [arXiv:1302.1069 [hep-ph]]; B. A. Arbuzov and I. V. Zaitsev, *Non-perturbative approach to the problem of anomalous FB asymmetry in top pair production at TEVATRON*, arXiv:1302.0663 [hep-ph]; X. Guo, T. Feng, S. Zhao, H.-W. Ke and X.-Q. Li, *Measuring Forward-Backward Asymmetry of $t\bar{t}$ and $b\bar{b}$ at Electron-Positron Colliders*, arXiv:1302.0485 [hep-ph].

[12] P. Skands, B. Webber and J. Winter, *QCD Coherence and the Top Quark Asymmetry*, JHEP **1207** (2012), 151, [arXiv:1205.1466 [hep-ph]].

[13] S. Dittmaier, P. Uwer and S. Weinzierl, *Phenomenological studies of top-pair production + jet at NLO*, 219–222,

arXiv:0905.2299 [hep-ph].
[14] K. Melnikov and M. Schulze, *NLO QCD corrections to top quark pair production in association with one hard jet at hadron colliders*, Nucl. Phys. **B840** (2010), 129–159, [arXiv:1004.3284 [hep-ph]].
[15] W. Hollik and D. Pagani, *The electroweak contribution to the top quark forward-backward asymmetry at the Tevatron*, Phys.Rev. **D84** (2011), 093003, [arXiv:1107.2606 [hep-ph]]; J. Kühn, A. Scharf and P. Uwer, *Weak Interactions in Top-Quark Pair Production at Hadron Colliders: An Update*, arXiv:1305.5773 [hep-ph].
[16] P. Bärnreuther, M. Czakon and A. Mitov, *Percent level precision physics at the Tevatron: first genuine NNLO QCD corrections to $q\bar{q} \to t\bar{t} + X$*, Phys.Rev.Lett. **109** (2012), 132001; M. Czakon and A. Mitov, *NNLO corrections to top-pair production at hadron colliders: the all-fermionic scattering channels*, JHEP **1212** (2012), 054, [arXiv:1207.0236 [hep-ph]]; M. Czakon and A. Mitov, *NNLO corrections to top pair production at hadron colliders: the quark-gluon reaction*, JHEP **1301** (2013), 080, [arXiv:1210.6832 [hep-ph]]; M. Czakon, P. Fiedler and A. Mitov, *The total top quark pair production cross-section at hadron colliders through $O(\alpha_S^4)$*, arXiv:1303.6254 [hep-ph].
[17] M. Beneke, P. Falgari and C. Schwinn, *Soft radiation in heavy-particle pair production: All-order colour structure and two-loop anomalous dimension*, Nucl.Phys. **B828** (2010), 69–101, [arXiv:0907.1443 [hep-ph]]; M. Czakon, A. Mitov and G. F. Sterman, *Threshold Resummation for Top-Pair Hadroproduction to Next-to-Next-to-Leading Log*, Phys.Rev. **D80** (2009), 074017, [arXiv:0907.1790 [hep-ph]]; V. Ahrens, A. Ferroglia, M. Neubert, B. D. Pecjak and L. L. Yang, *Precision predictions for the $t+\bar{t}$ production cross section at hadron colliders*, Phys.Lett. **B703** (2011), 135–141, [arXiv:1105.5824 [hep-ph]]; N. Kidonakis and B. D. Pecjak, *Top-quark production and QCD*, Eur.Phys.J. **C72** (2012), 2084, [arXiv:1108.6063 [hep-ph]]; M. Beneke, P. Falgari, S. Klein and C. Schwinn, *Hadronic top-quark pair production with NNLL threshold resummation*, Nucl.Phys. **B855** (2012), 695–741, [arXiv:1109.1536 [hep-ph]]; M. Cacciari, M. Czakon, M. Mangano, A. Mitov and P. Nason, *Top-pair production at hadron colliders with next-to-next-to-leading logarithmic soft-gluon resummation*, Phys.Lett. **B710** (2012), 612–622, [arXiv:1111.5869 [hep-ph]]; S. Moch, P. Uwer and A. Vogt, *On top-pair hadro-production at next-to-next-to-leading order*, Phys.Lett. **B714** (2012), 48–54, [arXiv:1203.6282 [hep-ph]].
[18] A. Kardos, C. Papadopoulos and Z. Trocsanyi, *Top quark pair production in association with a jet with NLO parton showering*, arXiv:1101.2672 [hep-ph].
[19] T. Gehrmann, S. Höche, F. Krauss, M. Schönherr and F. Siegert, *NLO QCD matrix elements + parton showers in e^+e^- →hadrons*, arXiv:1207.5031 [hep-ph]; S. Höche, F. Krauss, M. Schönherr and F. Siegert, *QCD matrix elements + parton showers: The NLO case*, arXiv:1207.5030 [hep-ph].
[20] T. Gleisberg, S. Höche, F. Krauss, A. Schälicke, S. Schumann and J. Winter, *SHERPA 1.α, a proof-of-concept version*, JHEP **02** (2004), 056, [hep-ph/0311263]; T. Gleisberg, S. Höche, F. Krauss, M. Schönherr, S. Schumann, F. Siegert and J. Winter, *Event generation with SHERPA 1.1*, JHEP **02** (2009), 007, [arXiv:0811.4622 [hep-ph]].
[21] G. Cullen, N. Greiner, G. Heinrich, G. Luisoni, P. Mastrolia, G. Ossola, T. Reiter and F. Tramontano, *Automated One-Loop Calculations with GoSam*, Eur.Phys.J. **C72** (2012), 1889, [arXiv:1111.2034 [hep-ph]]; G. Cullen, N. Greiner, G. Heinrich, G. Luisoni, P. Mastrolia, G. Ossola and T. Reiter, *GoSam: A program for automated one-loop Calculations*, arXiv:1111.6534 [hep-ph].
[22] P. Mastrolia, G. Ossola, T. Reiter and F. Tramontano, *Scattering AMplitudes from Unitarity-based Reduction Algorithm at the Integrand-level*, JHEP **1008** (2010), 080, [arXiv:1006.0710 [hep-ph]].
[23] G. Ossola, C. G. Papadopoulos and R. Pittau, *Reducing full one-loop amplitudes to scalar integrals at the integrand level*, Nucl. Phys. **B763** (2007), 147–169, [hep-ph/0609007]; R. Ellis, W. Giele and Z. Kunszt, *A numerical unitarity formalism for evaluating one-loop amplitudes*, JHEP **0803** (2008), 003, [arXiv:0708.2398 [hep-ph]].
[24] T. Binoth, J. P. Guillet, G. Heinrich, E. Pilon and T. Reiter, *Golem95: A numerical program to calculate one-loop tensor integrals with up to six external legs*, Comput. Phys. Commun. **180** (2009), 2317–2330, [arXiv:0810.0992 [hep-ph]]; G. Cullen, J. P. Guillet, G. Heinrich, T. Kleinschmidt, E. Pilon et al., *Golem95C: A library for one-loop integrals with complex masses*, Comput.Phys.Commun. **182** (2011), 2276–2284, [arXiv:1101.5595 [hep-ph]].
[25] G. Luisoni, M. Schönherr, F. Tramontano and J. Winter, in preparation.
[26] T. Binoth et al., *A proposal for a standard interface between Monte Carlo tools and one-loop programs*, Comput. Phys. Commun. **181** (2010), 1612–1622, [arXiv:1001.1307 [hep-ph]].
[27] S. Höche, F. Krauss, M. Schönherr and F. Siegert, *A critical appraisal of NLO+PS matching methods*, JHEP **09** (2012), 049, [arXiv:1111.1220 [hep-ph]].
[28] R. Frederix and S. Frixione, *Merging meets matching in MC@NLO*, JHEP **1212** (2012), 061, [arXiv:1209.6215 [hep-ph]].
[29] S. Catani and M. H. Seymour, *A general algorithm for calculating jet cross sections in NLO QCD*, Nucl. Phys. **B485** (1997), 291–419, [hep-ph/9605323].
[30] S. Catani, S. Dittmaier, M. H. Seymour and Z. Trocsanyi, *The dipole formalism for next-to-leading order QCD calculations with massive partons*, Nucl. Phys. **B627** (2002), 189–265, [hep-ph/0201036].
[31] S. Schumann and F. Krauss, *A parton shower algorithm based on Catani-Seymour dipole factorisation*, JHEP **03** (2008), 038, [arXiv:0709.1027 [hep-ph]].
[32] G. Marchesini and B. R. Webber, *Simulation of QCD Jets Including Soft Gluon Interference*, Nucl. Phys. **B238** (1984), 1.
[33] G. Marchesini and B. R. Webber, *Monte Carlo Simulation of General Hard Processes with Coherent QCD Radiation*, Nucl. Phys. **B310** (1988), 461.
[34] S. Catani, F. Krauss, R. Kuhn and B. R. Webber, *QCD matrix elements + parton showers*, JHEP **11** (2001), 063, [hep-ph/0109231]; F. Krauss, *Matrix elements and parton showers in hadronic interactions*, JHEP **0208** (2002), 015, [hep-ph/0205283].
[35] S. Höche, F. Krauss, S. Schumann and F. Siegert, *QCD matrix elements and truncated showers*, JHEP **05** (2009), 053, [arXiv:0903.1219 [hep-ph]].

[36] L. Lönnblad, *Correcting the colour-dipole cascade model with fixed order matrix elements*, JHEP **05** (2002), 046, [hep-ph/0112284].

[37] L. Lönnblad and S. Prestel, *Merging Multi-leg NLO Matrix Elements with Parton Showers*, JHEP **1303** (2013), 166, [arXiv:1211.7278 [hep-ph]].

[38] L. Lönnblad and S. Prestel, *Unitarising Matrix Element + Parton Shower merging*, JHEP **1302** (2013), 094, [arXiv:1211.4827 [hep-ph]]; S. Plätzer, *Controlling inclusive cross sections in parton shower + matrix element merging*, arXiv:1211.5467 [hep-ph].

[39] F. Krauss, R. Kuhn and G. Soff, *AMEGIC++ 1.0: A Matrix Element Generator In C++*, JHEP **02** (2002), 044, [hep-ph/0109036].

[40] T. Gleisberg and S. Höche, *Comix, a new matrix element generator*, JHEP **12** (2008), 039, [arXiv:0808.3674 [hep-ph]].

[41] T. Gleisberg and F. Krauss, *Automating dipole subtraction for QCD NLO calculations*, Eur. Phys. J. **C53** (2008), 501–523, [arXiv:0709.2881 [hep-ph]].

[42] S. Höche, S. Schumann and F. Siegert, *Hard photon production and matrix-element parton-shower merging*, Phys. Rev. **D81** (2010), 034026, [arXiv:0912.3501 [hep-ph]].

[43] S. Höche and M. Schönherr, *Uncertainties in NLO + parton shower matched simulations of inclusive jet and dijet production*, arXiv:1208.2815 [hep-ph].

[44] A. D. Martin, W. J. Stirling, R. S. Thorne and G. Watt, *Parton distributions for the LHC*, Eur. Phys. J. **C63** (2009), 189–295, [arXiv:0901.0002 [hep-ph]].

[45] S. Chatrchyan et al., The CMS collaboration, *Measurement of the charge asymmetry in top-quark pair production in proton-proton collisions at $\sqrt{s}$ = 7 TeV*, Phys.Lett. **B709** (2012), 28–49, [arXiv:1112.5100 [hep-ex]]; G. Aad et al., The ATLAS collaboration, *Measurement of the charge asymmetry in top quark pair production in pp collisions at $\sqrt{s}$ = 7 TeV using the ATLAS detector*, Eur.Phys.J. **C72** (2012), 2039, [arXiv:1203.4211 [hep-ex]]; S. Chatrchyan et al., The CMS collaboration, *Inclusive and differential measurements of the $t\bar{t}$ charge asymmetry in proton-proton collisions at 7 TeV*, Phys.Lett. **B717** (2012), 129–150, [arXiv:1207.0065 [hep-ex]].

[46] D. Krohn, T. Liu, J. Shelton and L.-T. Wang, *A Polarized View of the Top Asymmetry*, Phys.Rev. **D84** (2011), 074034, [arXiv:1105.3743 [hep-ph]]; A. Falkowski, G. Perez and M. Schmaltz, *Spinning the top quark*, Phys. Rev. D **87** (2013), 034041, [1110.3796]; E. L. Berger, Q.-H. Cao, C.-R. Chen, J.-H. Yu and H. Zhang, *Dynamical Origin of the Correlation between the Asymmetries A^t_{FB} and A^ℓ_{FB}*, arXiv:1111.3641 [hep-ph]; E. L. Berger, Q.-H. Cao, C.-R. Chen, J.-H. Yu and H. Zhang, *The Top Quark Production Asymmetries A^t_{FB} and A^ℓ_{FB}*, Phys.Rev.Lett. **108** (2012), 072002, [arXiv:1201.1790 [hep-ph]]; W. Bernreuther and Z.-G. Si, *Top quark and leptonic charge asymmetries for the Tevatron and LHC*, Phys.Rev. **D86** (2012), 034026, [arXiv:1205.6580 [hep-ph]]; A. Falkowski, M. L. Mangano, A. Martin, G. Perez and J. Winter, *Data driving the top quark forward–backward asymmetry with a lepton-based handle*, Phys.Rev. **D87** (2013), 034039, [arXiv:1212.4003 [hep-ph]].

[47] T. Carli, T. Gehrmann and S. Höche, *Hadronic final states in deep-inelastic scattering with SHERPA*, Eur. Phys. J. **C67** (2010), 73, [arXiv:0912.3715 [hep-ph]].

[48] A. van Hameren, *OneLOop: For the evaluation of one-loop scalar functions*, Comput.Phys.Commun. **182** (2011), 2427–2438, [arXiv:1007.4716 [hep-ph]].